Frequency-Hopped Space-Time Coded OFDM over Time-Varying Multipath Channel

Fangfang Cheng, Jiyu Jin(✉), Guiyue Jin, Peng Li, and Jun Mou

School of Information Science and Engineering, Dalian Polytechnic University, Dalian 116034, China
fangfangcheng25@163.com,
{jiyu.jin, guiyue.jin, lipeng, moujun}@dlpu.edu.cn

Abstract. In this paper, we proposed a frequency-hopped space-time coded orthogonal frequency-division multiplexing (FHST-OFDM) over time-varying multipath channels. Although OFDM is robust against frequency-selective fading channels, it is more vulnerable to the time-varying channels and has a higher peak-to-average power ratio (PAPR) than single-carrier systems. In space-time block coded OFDM (ST-OFDM), channel time variations cause not only the intertransmit-antenna interference (ITAI), but also the inter-carrier interference (ICI). In this paper, based on the analysis of the ITAI and ICI in ST-OFDM systems, the FHST-OFDM transmission scheme is proposed to reduce both ITAI, ICI, and PAPR simultaneously. By combining the Alamouti scheme and the frequency hopping, full data rate and frequency diversity can be achieved by the proposed FHST-OFDM over the time-varying multipath channels. Finally, simulation shows that the proposed FHST-OFDM scheme gets better performance over time varying channels.

Keywords: STBC · OFDM · Intercarrier interference (ICI)
Intertransmit-antenna interference (ITAI) · Time-varying channel

1 Introduction

In order to eliminate the detrimental influence of the channel fading and increase spectrum efficiency, both of the transmit diversity and the orthogonal frequency division multiplexing (OFDM) technologies have drawn a lot of attentions and exhibited great advantages in the next generation wireless communication systems.

Recently, transmit diversity has been studied extensively as a method of overcoming the detrimental effects of wireless fading channels because it is relatively easy to implement and multiple antennas at the base station are often available. One attractive approach of implementing transmit diversity is space-time block codes (STBCs) [1–3]. However, the orthogonal space-time block code (OSTBC) results in data rate loss if more than two transmit antennas are used [2]. The quasi-orthogonal space-time block code (QOSTBC) was proposed in [4, 5] to achieve full data rate at the cost of performance loss. Moreover, STBC are typically designed assuming that channel is quasi-static fading. However, in practice, the time-varying channel will

X. Gu et al. (Eds.): MLICOM 2017, Part II, LNICST 227, pp. 634–646, 2018.
https://doi.org/10.1007/978-3-319-73447-7_68

destroy the orthogonality of signals among the transmit antennas and result in intertransmit-antenna interference (ITAI) in the STBCs.

Multi-antennas can be combined with OFDM to achieve spatial diversity and/or to increase spectral efficiency through spatial multiplexing. for the multi-antenna OFDM systems in frequency-selective channels, STBC schemes must be extended to include frequency element, forming space-time block coded OFDM (ST-OFDM) [6–9]. Similar to single antenna OFDM, ST-OFDM is also sensitive to the Doppler shift and frequency offsets that destroy the orthogonality among the subcarriers. In the OFDM systems with N_s subcarriers, the OFDM symbol duration is N_s, the number of subcarriers, times the modulated sampling period. Consequently, ITAI caused by channel time variations in ST-OFDM systems is more pronounced than that in single-carrier STBC systems. Interference cancellation schemes for ST-/QOST-OFDM over fast varying channel were proposed in [10–14] to mitigate the ITAI and/or Intercarrier interference (ICI). However, these interference cancellation schemes increase the computational load at the receiver.

The performance of a mobile communication system heavily relies on how well the system is designed to overcome the time-varying channel. In this paper, based on the analysis of the ITAI and ICI in ST-OFDM systems, a simple FHST-OFDM transmission scheme with four transmit antennas is proposed to mitigate the ITAI and ICI. Additionally, the peak-to-average power ratio (PAPR) is also been suppressed. In the proposed FHST-OFDM scheme, Alamouti STBC scheme and frequency hopping are adopted to provide full data rate and frequency diversity over the time-varying multipath channels. By using frequency hopping, only $N_s/2$ subcarriers are active in each time slot for each antenna. Therefore, the proposed FHST-OFDM experiences less ICI and it has a lower PAPR.

This paper is organized as follows. The system description is provided in Sect. 2. The proposed FHST-OFDM is derived in Sect. 3. Section 4 presents the simulation results and Sect. 5 concludes this paper.

Notation: In this paper, a boldface letter denotes a vector or matrix, which will be clear from the context; I_M denotes an $M \times M$ identity matrix. The superscript $(\cdot)^*$, $(\cdot)^T$, and $(\cdot)^H$ denote the complex conjugate, the transpose and the Hermitian transpose operators, respectively. $|\cdot|$, E$(\cdot)$ and var$(\cdot)$ represents absolute value, expectation and variance operators, respectively. *diag*$(\cdot)$ denotes the diagonal parts of a matrix. $\|\cdot\|_F$ and *tr*$(\cdot)$ denote the Frobenius norm and the trace of a matrix, respectively.

2 System Description

We focus on an ST-OFDM system with P transmit antennas, one receive antenna, and N_s subcarriers in the time-varying multipath channels. The input sequence $\{a(i), i = 0, \ldots, N_s P - 1\}$ is serial-to-parallel converted into P sequences, each of length N_s, as

$$a_p(k) = a(k + (p-1)N_s), \quad \text{for } p = 1, \ldots, P, \text{ and } k = 0, \ldots, N_s - 1. \tag{1}$$

Each sequences a_p (k) is then serial-to-parallel converted and mapped into the space-time coded matrix according to the ST-OFDM scheme.

Taking the inverse discrete Fourier transform (IDFT), the $N_s \times 1$ complex vector for each transmit antenna is converted into time-domain. The time-domain signals transmitted from the p-th antenna during the q-th OFDM symbol period can be expressed by

$$x_{p,\,q}(m) = \sum_{k=0}^{N_s-1} b_{p,\,q}(k) \cdot e^{j\frac{2\pi}{N_s}mk}, \quad m = 0, \ldots, N_s - 1, \text{ and } q = 1, \ldots, Q, \tag{2}$$

where $b_{p,q}(k)$ is the space-time encoded symbol for the p-th transmit antenna during the q-th symbol period on the k-th subcarrier, and Q denotes the block size of the space-time code. After the cyclic prefixes are added, the OFDM symbols are transmitted.

Since the channel is time-varying, the relationship between the channel coefficients for path l (l = 0, …, L − 1) of antenna p at times nT_s (T_s is the sampling interval) and $(n + m)$ T_s during the q-th OFDM symbol period can be described by using the first-order autoregressive model as in [15, 16].

$$h_{p,\,q}(n+m, l) = \alpha_m h_{p,\,q}(n,\ l) + \beta_{p,\,q}(n+m,\ l), \tag{3}$$

where

$$\alpha_m = J_0(2\pi \cdot m f_d T_s), \tag{4}$$

and f_d is the Doppler shift, $J_0(\cdot)$ is the zeroth-order Bessel function of the first kind, $\beta_{p,q}$ (n, l) are independent (for different indexes p, q, l, and n) complex Gaussian random variables with zero mean and variance

$$\sigma_\beta^2 = \sigma_l^2\left(1 - \alpha_m^2\right), \tag{5}$$

where σ_l^2 denotes the variance of the l-th path of the channel.

The received signal at the sampling time n can be given as

$$y_q(n) = \sum_{p=1}^{P} \sum_{l=0}^{L-1} h_{p,\,q}(n,\ l) x_{p,\,q}(n - \tau_l) + w_q(n), \tag{6}$$

where τ_l denotes the delay of the l-th path, $w_q(n)$ is complex additive white Gaussian noise (AWGN) with zero mean and variance of σ^2.

At the receiver, after removing the cyclic prefixes and performing FFT, the received signal on the m-th subcarrier can be given as

$$r_q(m) = \sum_{p=1}^{P} \sum_{k=0}^{N_s-1} \varphi_{p,q}(m,\, k) b_{p,q}(k) e^{-j\frac{2\pi}{N_s}mk} + v_q(m), \quad k = 0, \ldots, N_s - 1 \text{ and } q = 1, \ldots, Q, \tag{7}$$

where $v_q\,(m)$ denotes the FFT of additive white Gaussian noise, and

$$\varphi_{p,q}(m,\, k) = \sum_{l=0}^{L-1} \eta_{p,q,l}(m-k) e^{-j\frac{2\pi}{N_s}kl}, \tag{8}$$

$$\eta_{p,q,l}(m-k) = \frac{1}{N_s} \sum_{n=0}^{N_s-1} h_{p,q}(n,\, l) e^{-j\frac{2\pi}{N_s}(m-k)n}, \tag{9}$$

The notation $\eta_{p,q,l}(m - k)$ represents the FFT of the l-th path component between the p-th transmit antenna and the receive antenna during the q-th symbol period. Note that $\varphi_{p,q}(m,\, k)$, for $k \neq m$, denotes the ICI from the k-th subchannel to the m-th subchannel for the p-th transmit antenna, and $\varphi_{p,q}(m, k) = \varphi_{p,q}(m)$ for $k = m$. The more detailed interpretation of $\eta_{p,q,l}(m - k)$ and $\varphi_{p,q}(m, k)$ is provided in [17].

The received signals can be expressed in matrix form as

$$\mathbf{R}(m) = \mathbf{H}(m)\mathbf{A}(m) + \sum_{k=0,\, k\neq m}^{N_s-1} \mathbf{H}(m,\, k)\mathbf{A}(k) + \mathbf{V}(m)\,, \quad \text{for } m = 0, \ldots, N_s - 1, \tag{10}$$

where $\mathbf{R}(m) = \left[r_1(m),\, r_2^*(m),\, \ldots, r_{Q-1}(m),\, r_Q^*(m)\right]^T$, $\mathbf{A}(m) = [a_1(m),\, \ldots, a_p(m),\, \ldots,$ $a_P(m)]^T$, and $\mathbf{V}(m) = \left[v_1(m),\, v_2^*(m),\, \ldots, v_{Q-1}(m),\, v_Q^*(m)\right]^T$, $\mathbf{H}(m)$ is the equivalent channel matrix with dimensions $Q \times P$. The second term on the right-hand side of (10) represents the ICI, and channel time-variations in $\mathbf{H}(m)$ induce ITAI.

$$\mathbf{C}_{\mathrm{ITAI}}(m) = \mathbf{H}^H(m)\mathbf{H}(m) - \boldsymbol{\rho}(m), \tag{11}$$

where

$$\boldsymbol{\rho}(m) = diag\left(\mathbf{H}^H(m)\mathbf{H}(m)\right). \tag{12}$$

3 Frequency-Hopped Space-Time Code OFDM

In the ST-OFDM systems, the frequency-selective channel is converted into a collection of parallel frequency flat fading subchannels. Therefore, a space-time block code can be applied for each subcarrier. In general, the detector assumes that the channel does not change during a space-time coded OFDM symbol block. This is a

critical restriction for OFDM compared to single carrier systems since the OFDM symbol duration is N_s times larger than the symbol duration in single carrier system. In ST-OFDM, the time-varying channels cause not only ITAI but also ICI among different subcarriers. Consequently, the performance of ST-OFDM will become poor under fast fading environments.

In this section, we present an FHST-OFDM equipped with four transmit antennas over time-varying channels. The block diagram of FHST-OFDM is given in Fig. 1. At the transmitter, the modulated symbols are space-time coded by using two STBC encoders. For antenna 1 and antenna 2, during the first and second symbol durations, the space-time coded symbols are transmitted on odd subcarriers, and during the third and fourth symbol durations, the space-time coded symbols are transmitted on even subcarriers. Contrarily, for antenna 3 and antenna 4, during the first and second symbol durations, the space-time coded symbols are transmitted on even subcarriers, and during the third and fourth symbol durations, the space-time coded symbols are transmitted on odd subcarriers. The space-time coded symbols are modulated by IFFT into OFDM symbols. After adding cyclic prefixes, the OFDM symbols are transmitted.

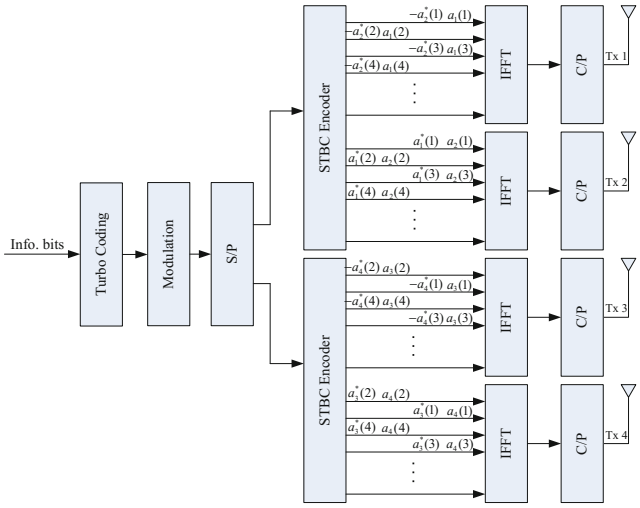

Fig. 1. Frequency hopped space-time coded OFDM scheme with 4 transmit antennas.

At the receiver, after removing the cyclic prefixes and performing FFT, the received signal vector on the even and odd subcarriers can be given as

$$\mathbf{R_e}(m) = \mathbf{H}_\mathrm{e}(m)\mathbf{A}_\mathrm{e}(m) + \sum_{k=0}^{N_s-2} \mathbf{H}_\mathrm{e}(m,\, k)\mathbf{A}_\mathrm{e}(k) + \mathbf{V}_\mathrm{e}(m), \qquad m,\, k = 0, 2, \ldots, N_s - 2 \tag{13}$$

$$\mathbf{R}_{\mathrm{o}}(m) = \mathbf{H}_{\mathrm{o}}(m)\mathbf{A}_{\mathrm{o}}(m) + \sum_{k=1}^{N_s-1} \mathbf{H}_{\mathrm{o}}(m,k)\mathbf{A}_{\mathrm{o}}(k) + \mathbf{V}_{\mathrm{o}}(m), \quad m,\ k = 1, 3, \ldots, N_s - 1 \tag{14}$$

where $\mathbf{H}_{\mathrm{e}}(m)$ and $\mathbf{H}_{\mathrm{o}}(m)$ are the equivalent channel matrices on the even and odd subcarriers, respectively, in the frequency domain, $\mathbf{A}_{\mathrm{e}}(m)/\mathbf{A}_{\mathrm{o}}(m)$ and $\mathbf{V}_{\mathrm{e}}(m)/\mathbf{V}_{\mathrm{o}}(m)$ are the transmitted signal and the noise vectors on the even/odd subcarriers.

3.1 ITAI Caused by Time-Varying Channels

As shown in Fig. 1, since the even and odd subcarriers on the different antennas are used alternately, there is no interference for the space-time coded symbols between two STBC encoders. However, in the time-varying channel, the channel coefficients will change in time, which may cause ITAI (11). Considering the time-varying characteristics of the channel, we analyze the ITAI of the proposed FHST-OFDM.

The equivalent channel matrix in (13) and (14) can be given as

$$\mathbf{H}_{\mathrm{e/o}}(m) = \begin{pmatrix} \varphi_{p,1}(m) & \varphi_{p+1,1}(m) \\ -\varphi^*_{p+1,2}(m) & \varphi^*_{p,2}(m) \end{pmatrix}, \quad p = 1, 3 \tag{15}$$

where $\varphi_{p,q}(m)$ ($\varphi_{p,q}(m,\ k) = \varphi_{p,q}(m)$, when $k = m$) denotes the channel frequency response on the m-th (even/odd) subcarrier for the p-th transmit antenna and the q-th ($q = 1, 2$) symbol time, and

$$\varphi_{p,2}(m) = \gamma \cdot \varphi_{p,1}(m) + \varepsilon_{p,1}, \tag{16}$$

where $\varepsilon_{p,1}$ are independent complex Gaussian random variables with zero mean and variance

$$\sigma_{\varepsilon}^2 = 1 - |\gamma|^2, \tag{17}$$

and the channel correlation factor γ is given as

$$\gamma = J_0(2\pi \cdot f_d(N_s + c)T_s), \tag{18}$$

where c denotes the length of cyclic prefix.

According to (15), we represent (11) as (19)

$$\begin{aligned} \mathbf{C}_{\mathrm{ITAI}}^{\mathrm{FHST}}(m) &= \begin{pmatrix} |\varphi_{p,1}(m)|^2 + |\varphi_{p+1,2}(m)|^2 & \varphi^*_{p,1}(m)\varphi_{p+1,1}(m) - \varphi^*_{p,2}(m)\varphi_{p+1,2}(m) \\ \varphi_{p,1}(m)\varphi^*_{p+1,1}(m) - \varphi_{p,2}(m)\varphi^*_{p+1,2}(m) & |\varphi_{p+1,1}(m)|^2 + |\varphi_{p,2}(m)|^2 \end{pmatrix} \\ &\quad - \begin{pmatrix} |\varphi_{p,1}(m)|^2 + |\varphi_{p+1,2}(m)|^2 & 0 \\ 0 & |\varphi_{p+1,1}(m)|^2 + |\varphi_{p,2}(m)|^2 \end{pmatrix} \\ &= \begin{pmatrix} 0 & \varphi^*_{p,1}(m)\varphi_{p+1,1}(m) - \varphi^*_{p,2}(m)\varphi_{p+1,2}(m) \\ \varphi_{p,1}(m)\varphi^*_{p+1,1}(m) - \varphi_{p,2}(m)\varphi^*_{p+1,2}(m) & 0 \end{pmatrix} \\ &= \begin{pmatrix} 0 & \mu_{12}(m) \\ \mu_{21}(m) & 0 \end{pmatrix}. \end{aligned} \tag{19}$$

Substituting (16) into (19), the magnitude of interference $\mu_{1,2}(m)$, $\mu_{2,1}(m)$ in (19) can be given as

$$\begin{aligned}\mu_{1,2}(m) &= \varphi^*_{p,1}(m)\varphi_{p+1,1}(m) \\ &\quad - \left[\gamma^*\varphi^*_{p,1}(m) + \varepsilon^*_{p+1}(m)\right]\left[\gamma\varphi_{p+1,1}(m) + \varepsilon_{p+1,1}(m)\right],\end{aligned} \tag{20}$$

$$\begin{aligned}\mu_{2,1}(m) &= \varphi_{p,1}(m)\varphi^*_{p+1,1}(m) \\ &\quad - \left[\gamma\varphi_{p,1}(m) + \varepsilon_{p,1}(m)\right]\left[\gamma^*\varphi^*_{p+1,1}(m) + \varepsilon^*_{p+1,1}(m)\right],\end{aligned} \tag{21}$$

where $\varepsilon_{p,q}(m)$ (q = 1, 2) has zero-mean and variance $1 - |\gamma|^2$, and we assume that $\varphi_{p,q}(m)$ is a complex Gaussian process with zero-mean and unit-variance. The variance of $\mu_{1,2}(m)$ and $\mu_{2,1}(m)$ can be given as

$$\mathrm{var}\left(\mu_{1,2}(m)\right) = \mathrm{var}\left(\mu_{2,1}(m)\right) = 2\left(1 - |\gamma|^2\right), \tag{22}$$

The variance of $|\varphi_{p,1}(m)|^2 + |\varphi_{p+1,2}(m)|^2$ and $|\varphi_{p+1,1}(m)|^2 + |\varphi_{p,2}(m)|^2$ in (19) can be given as

$$\begin{aligned}&\mathrm{var}\left(\left|\varphi_{p,1}(m)\right|^2 + \left|\varphi_{p+1,2}(m)\right|^2\right) \\ &= \mathrm{var}\left(\left|\varphi_{p+1,1}(m)\right|^2 + \left|\varphi_{p,2}(m)\right|^2\right) = 2.\end{aligned} \tag{23}$$

Therefore, at each subcarrier, the signal to ITAI ratio of the FHST-OFDM is

$$\mathrm{SIR}^{\mathrm{FHST}}_{\mathrm{ITAI}} = 1/\left(1 - |\gamma|^2\right), \tag{24}$$

According to (18) and (24), the $\mathrm{SIR}^{\mathrm{FHST}}_{\mathrm{ITAI}}$ is the function of f_d and T_s, as

$$\mathrm{SIR}^{\mathrm{FHST}}_{\mathrm{ITAI}} = f_{\mathrm{FHST}}(f_d, T_s). \tag{25}$$

The equivalent channel matrix of QOST-OFDM can be given as

$$\mathbf{H}_{\mathrm{QOST}} = \begin{pmatrix} \varphi_{1,1}(m) & \varphi_{2,1}(m) & \varphi_{3,1}(m) & \varphi_{4,1}(m) \\ -\varphi^*_{2,2}(m) & \varphi^*_{1,2}(m) & -\varphi^*_{2,2}(m) & \varphi^*_{3,2}(m) \\ -\varphi^*_{3,3}(m) & -\varphi^*_{4,3}(m) & \varphi^*_{1,3}(m) & \varphi^*_{2,3}(m) \\ \varphi_{4,4}(m) & -\varphi_{3,4}(m) & -\varphi_{2,4}(m) & \varphi_{1,4}(m) \end{pmatrix}. \tag{26}$$

Similar to the above analysis, with four transmit antennas, the signal to ITAI ratio of QOST-OFDM at each subcarrier can be given as

$$\mathrm{SIR}^{\mathrm{FHST}}_{\mathrm{ITAI}} = 1/\left(2 - \gamma^2 - \gamma^4\right) = f_{\mathrm{QOST}}(f_d, T_s). \tag{27}$$

For QOST-OFDM, since the interference caused by the code structure is manipulated by a pairwise maximum-likelihood (ML) decoding scheme [4], only the interference caused by time-varying is considered in (27).

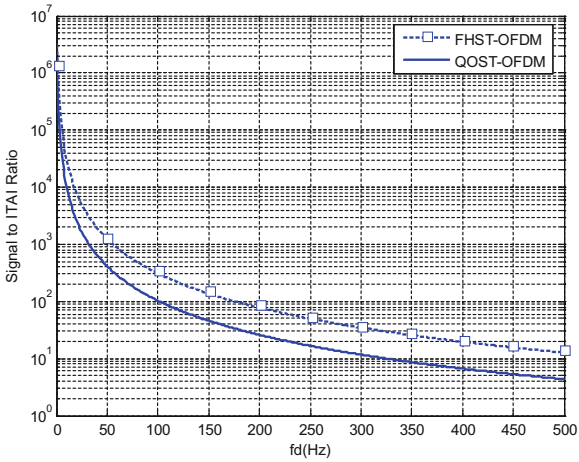

Fig. 2. Signal-to-ITAI ratio versus f_d.

As the functions of f_d, $\mathrm{SIR}_{\mathrm{ITAI}}^{\mathrm{FHST}}$ and $\mathrm{SIR}_{\mathrm{ITAI}}^{\mathrm{QOST}}$ are compared in Fig. 2. As shown in Fig. 2, in time-varying channels, as f_d increases, the signal-to-ITAI ratio of QOST-OFDM decreases more rapidly than that of the proposed FHST-OFDM scheme. Compared to QOST-OFDM, the block size of the proposed FHST-OFDM is two instead of four. Therefore the proposed FHST-OFDM scheme is less sensitive to the time-varying channels than the QOST-OFDM, and it obtains better performance than QOST-OFDM over time-varying multipath channels.

$$
\begin{aligned}
\mathrm{SIR}_{\mathrm{ICI,e}}^{\mathrm{FHST}} &= \frac{E\left[\left\|\mathbf{H}_{\mathrm{e}}(m)\mathbf{A}_{\mathrm{e}}(m)\right\|_F^2\right]}{E\left[\left\|\sum_{k=0,\,k\neq m}^{N_s-2}\mathbf{H}_{\mathrm{e}}(m,k)\mathbf{A}_{\mathrm{e}}(m)\right\|_F^2\right]} \\
&= \frac{tr\left(E\left[\mathbf{H}_{\mathrm{e}}(m)\mathbf{A}_{\mathrm{e}}(m)\mathbf{A}_{\mathrm{e}}^H(m)\mathbf{H}_{\mathrm{e}}^H(m)\right]\right)}{tr\left(E\left[\left(\sum_{k=0,\,k\neq m}^{N_s-2}\mathbf{H}_{\mathrm{e}}(m,\,k)\mathbf{A}_{\mathrm{e}}(m)\right)\left(\sum_{k=0,k\neq m}^{N_s-2}\mathbf{H}_{\mathrm{e}}(m,\,k)\mathbf{A}_{\mathrm{e}}(m)\right)^H\right]\right)} \\
&= \frac{E[\boldsymbol{\rho}_{\mathrm{FHST}}(m)]}{tr\left(E\left[\left(\sum_{k=0,\,k\neq m}^{N_s-2}\mathbf{H}_{\mathrm{e}}(m,\,k)\mathbf{A}_{\mathrm{e}}(m)\right)\left(\sum_{k=0,\,k\neq m}^{N_s-2}\mathbf{H}_{\mathrm{e}}(m,\,k)\mathbf{A}_{\mathrm{e}}(m)\right)^H\right]\right)} \\
&= \frac{E\left[\sum_{q=1}^{2}\sum_{p=1}^{2}\left|\varphi_{p,\,q}(m)\right|^2\right]}{E\left[\sum_{k=0,\,k\neq m}^{N_s-2}\sum_{q=1}^{2}\sum_{p=1}^{2}\left|\varphi_{p,\,q}(m)\right|^2\right]}, \qquad m,\,k=0,\,2,\ldots,N_s-2,
\end{aligned}
\tag{28}
$$

and

$$\mathrm{SIR}_{\mathrm{ICI,o}}^{\mathrm{FHST}} = \frac{E\left[\sum_{q=1}^{2}\sum_{p=1}^{2}\left|\varphi_{p,q}(m)\right|^2\right]}{E\left[\sum_{k=1,k\neq m}^{N_s-1}\sum_{q=1}^{2}\sum_{p=1}^{2}\left|\varphi_{p,q}(m)\right|^2\right]}, \qquad m,k = 1,3,\ldots,N_s-1, \tag{29}$$

respectively, and

$$\mathrm{SIR}_{\mathrm{ICI}}^{\mathrm{FHST}} = \mathrm{SIR}_{\mathrm{ICI,e}}^{\mathrm{FHST}} = \mathrm{SIR}_{\mathrm{ICI,o}}^{FHST}. \tag{30}$$

3.2 ICI Caused by a Time-Varying Channel

Compared with QOST-OFDM, the proposed FHST-OFDM uses half subcarriers and they are spaced twice as far apart. In each time slot, only $N_s/2$ subcarriers are used in FHST-OFDM, so we can reduce the interference from adjacent subcarriers. Hence, the proposed FHST-OFDM experiences less ICI than the QOST-OFDM.

When the channel is time-varying, channel variation within an OFDM symbol gives rise to ICI as shown in (10). From (10), the signal to ICI ratio of the proposed FHST-OFDM at each even and odd subcarrier can be given (28) and (29) at the bottom of the previous page.

According to (10) and (24), the signal to ICI of QOST-OFDM can be given as

$$\begin{aligned}
\mathrm{SIR}_{\mathrm{ICI}}^{\mathrm{QOST}} &= \frac{E\left[\left\|\mathbf{H}(m)\mathbf{A}_Q(m)\right\|_F^2\right]}{E\left[\left\|\sum_{k=0,k\neq m}^{N_s-1}\mathbf{H}(m,k)\mathbf{A}_Q(m)\right\|_F^2\right]} \\
&= \frac{tr\left(E\left[\mathbf{H}(m)\mathbf{A}_Q(m)\mathbf{A}_Q^H(m)\mathbf{H}^H(m)\right]\right)}{tr\left(E\left[\left(\sum_{k=0,k\neq m}^{N_s-1}\mathbf{H}(m,k)\mathbf{A}_Q(m)\right)\left(\sum_{k=0,k\neq m}^{N_s-1}\mathbf{H}(m,k)\mathbf{A}_Q(m)\right)^H\right]\right)} \\
&= \frac{E\left[\boldsymbol{\rho}_{\mathrm{QOST}}(m)\right]}{tr\left(E\left[\left(\sum_{k=0,k\neq m}^{N_s-1}\mathbf{H}(m,k)\mathbf{A}_Q(m)\right)\left(\sum_{k=0,k\neq m}^{N_s-1}\mathbf{H}(m,k)\mathbf{A}_Q(m)\right)^H\right]\right)} \\
&= \frac{E\left[\sum_{q=1}^{4}\sum_{p=1}^{4}\left|\varphi_{p,q}(m)\right|^2\right]}{E\left[\sum_{k=0,k\neq m}^{N_s-1}\sum_{q=1}^{4}\sum_{p=1}^{4}\left|\varphi_{p,q}(m)\right|^2\right]}.
\end{aligned} \tag{31}$$

Since only $N_s/2$ subcarriers are used in the proposed FHST-OFDM, with (30) and (31), we have

$$\frac{\mathrm{SIR}_{\mathrm{ICI}}^{\mathrm{FHST}}}{\mathrm{SIR}_{\mathrm{ICI}}^{\mathrm{QOST}}} = 2. \tag{32}$$

the signal to ICI ratio of the FHST-OFDM is two times that of QOST-OFDM.

3.3 PAPR Reduction

One of drawbacks of the OFDM system is the PAPR. Since the complex baseband OFDM signal is the combination of many sinusoids with different frequencies, the instantaneous power of the resulting signal may be larger than the average power of the OFDM signal, so the signal exhibits high peaks. When the fluctuant signal exceeds the linear region of a high power amplifier (HPA), saturation caused by the large peaks will induce intermodulation distortion clipping noise. This distortion deteriorates bit error rate (BER) performance and causes spectral leaking, resulting in out-band interference [18].

PAPR is defined as the ratio of the peak power to the average power of the OFDM signal, and it is given by

$$PAPR = 10\ \log_{10}\left(\frac{P_{PEAK}}{P_{AVG}}\right) 10\ \log_{10} N_s \quad (\mathrm{dB}). \tag{33}$$

where P_{PEAK} and P_{AVG} is the peak power and average power, respectively. In the proposed FHST-OFDM, at each time slot, only $N_s/2$ subcarriers are used. The peak and average power of the FHST-OFDM is $N_s^2/4$ (W), and $N_s/2$ (W), respectively. Therefore, PAPR reduction achieved by the proposed FHST-OFDM can be deduced as

$$PAPR_{RD} = 10\log_{10} N_s - 10\log_{10}\left(\frac{N_s^2/4}{N_s/2}\right) = 3 \quad (\mathrm{dB}). \tag{34}$$

4 Simulation Results

In this section, we demonstrate the performance through computer simulations. Simulations are carried out based on the ITU channel model as shown in Table 1. We assume that the OFDM systems equip four transmit antennas and one receive antenna, and employ the quaternary phase-shift keying (QPSK) modulation. The turbo coding with the channel code rate $1/2$, the constraint length of 4 bits, and 8 iterations are considered in our simulations. The available channel bandwidth is 10 MHz, which is divided into 1024 tones, and we use a 1024-point IFFT and a 2.3 GHz center frequency. Moreover, we assume that perfect channel state information (CSI) is available at the receiver, and the transmit antennas are separated sufficiently.

In Fig. 3, we compare the proposed FHST-OFDM and QOST-OFDM with vehicular speed v = 5 km/h and v = 60 km/h. Alamouti decoding scheme [1] is used for FHST-OFDM and a pairwise ML decoding scheme [4] is used for QOST-OFDM, respectively. For v = 5 km/h, the FHST-OFDM outperforms the QOST-OFDM about 2.5 dB in the case of BER = 10^{-4}. At a high signal-to-noise ratio (SNR), the signal to interference ratio (SIR) is the dominant factor to the system performance. Since the proposed FHST-OFDM suffers less ITAI and ICI than the QOST-OFDM, it outperforms QOST-OFDM especially in the high SNR region. When SNR > 20 dB, the QOST-OFDM approaches saturation due to the effect of the SIR. As mentioned above, the proposed FHST-OFDM suffers less ITAI and ICI than QOST-OFDM due to the smaller block size and frequency hopping (only $N_s/2$ subcarriers are used in each time slot), so a larger v makes the QOST-OFDM more vulnerable to time variations of the channel coefficients. As shown in Fig. 3, at v = 60 km/h, the BER performance of the QOST-OFDM is degraded more rapidly than that of the proposed FHST-OFDM.

Table 1. ITU vehicular A channel model

Relative delay (ns)	0	310	710	1090	1730	2510
Power delay profile (dB)	0	−1.0	−9.0	−10.0	−15.0	−20.0

Figure 4 compares the BER performance of the proposed FHST-OFDM and QOST-OFDM when the decision feedback equalizer (DFE) is used to perform interference cancellation in the receiver. As shown in Fig. 4, at v = 60 km/h, the proposed FHST-OFDM gets about 5.5 dB of performance gain compared to QOST-OFDM.

It should be mentioned that the frequency response might not be constant over N_s subcarriers in a multipath channel environment. Therefore, the proposed FHST-OFDM

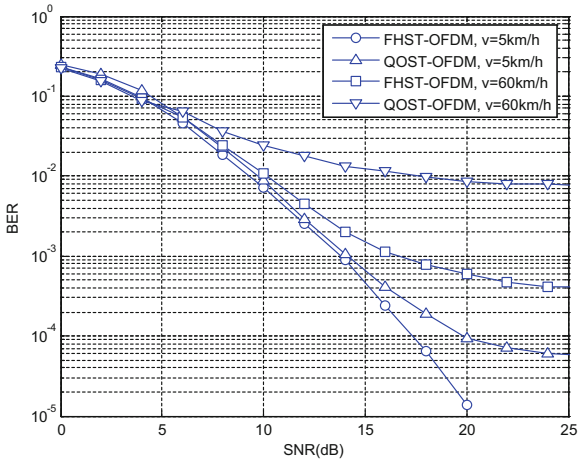

Fig. 3. BER performance for the proposed FHST-OFDM and QOST-OFDM with conventional decoding schemes.

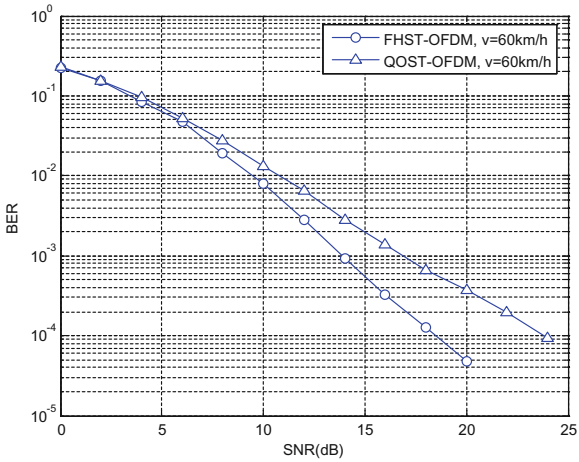

Fig. 4. BER performance for the proposed FHST-OFDM and QOST-OFDM with DFE at the receiver.

not only reduces the interference, but also achieves frequency diversity by using frequency hopping. Moreover, the FHST-OFDM can achieve a 3 dB PAPR reduction compared to QOST-OFDM since only $N_s/2$ subcarriers are used in each time slot.

5 Conclusion

In the ST-OFDM systems, time varying channel cause both the ITAI and ICI, which significantly degrade the BER performance. In this paper, we analyzed ITAI and ICI caused by channel variation, and a FHST-OFDM has been proposed. Compared with QOST-OFDM, the proposed FHST-OFDM is more robust against the time-varying channel. Frequency diversity can also be obtained over the multipath channel environment, and the proposed scheme gets lower PAPR than QOST-OFDM. Furthermore, since the proposed FHST-OFDM is a simple transmission scheme and no additional manipulation is needed at the receiver, it is attractive in low cost scenarios, such as the handset in the uplink of cellular networks.

Acknowledgements. This work supported by the Provincial Natural Science Foundation of Liaoning (Grant Nos. 20170540060 and 2015020031), Liaoning Provincial Department of Education Research Project (L2015043).

References

1. Alamouti, S.M.: A simple transmit diversity technique for wireless communications. IEEE J. Sel. Areas Commun. **16**(8), 1451–1458 (1998)
2. Tarokh, V., Jafarfarni, H., Calderband, A.R.: Space-time block codes from orthogonal designs. IEEE Trans. Inf. Theory **45**(5), 1456–1467 (1999)

3. Tarokh, V., Jafarkarni, H., Calderband, A.R.: Space-time block coding for wireless communications: performance results. IEEE J. Sel. Areas Commun. **17**(3), 451–460 (1987)
4. Jafarkarni, H.: A quasi-orthogonal space-time block code. IEEE Trans. Commun. **49**(1), 1–4 (2001)
5. Pham, V.B., Sheng, W.X.: No-zero-entry full diversity space-time block codes with linear receivers. Ann. Telecommun. **70**(1), 73–81 (2015)
6. Zhang, J., Zhang, M.: Error control coded space-time block coding for frequency-selective fading channels. In: First International Workshop On Education Technology and Computer Science, 2009, ETCS 2009, Wuhan, Hubei, China, March, pp. 923–926 (2009)
7. Liu, Z., Xin, Y., Giannakis, G.B.: Space-time-frequency coded OFDM over frequency-selective fading channels. IEEE Trans. Signal Process. **50**(10), 2465–2476 (2015)
8. Mudulodu, S., Paulraj, A.: A transmit diversity scheme for frequency selective fading channels. In: Proceedings of Globecom, vol. 2, pp. 1089–1093, November 2000
9. Lin, L.: Space-time block code design for Asymmetric-OFDM systems. In: Globecom Workshops 2012 IEEE, Anaheim, USA, pp. 204–209, December 2012
10. Groh, I., Dammann, A., Gentner, C.: Efficient inter-carrier interference mitigation for pilot-aided channel estimation in OFDM mobile systems. In: Vehicular Technology Conference (VTC Spring), 2011 IEEE 73rd, Yokohama, Japan, pp. 1–5, July. 2011
11. Stamoulis, A., Diggavi, S.N., Al-Dhahir, N.: Inter-carrier interference in MIMO OFDM. IEEE Trans. Signal Process. **50**(10), 2451–2464 (2002)
12. Chiu, Y.J., Chen, C.S., Chang, T.W.: Joint channel estimation and ISI47;ICI cancellation for MIMO OFDM systems. Int. J. Ad Hoc Ubiquitous Comput. **7**(2), 137–142 (2011)
13. Kim, J., Heath Jr., R.W., Power, E.J.: Receiver designs for Alamouti coded OFDM systems in fast fading channels. IEEE Trans. Commun. **4**(2), 550–559 (2005)
14. Zhang, Y., Liu, H.: Impact of time-selective fading on the performance of quasi-orthogonal space-time-coded OFDM systems. IEEE Trans. Commun. **54**, 251–260 (2006)
15. Tran, T.A., Sesay, A.B.: A generalized simplified ML decoder of orthogonal space-time block code for wireless communications over time-selective fading channels. In: Proceedings of IEEE Vehicular Technology Conference, pp. 1911–1915 (2002)
16. Ismail, B., Suvarna, M.: Estimation of linear regression model with correlated regressors in the presence of autocorrelation. Int. J. Stat. Appl. **6**(2), 35–39 (2016)
17. Hou, W.S., Chen, B.S.: ICI cancellation for OFDM communication systems in time-varying multipath fading channels. IEEE Press **4**(5), 2100–2110 (2005)
18. Miranda, J.P., Melgarejo, D., Mathilde, F.: Narrowband interference suppression in long term evolution systems. In: IEEE International Symposium on Personal, vol. 75, no. 4, pp. 64–72, June 2015